Measuring of velocity and temperature field in a model of reactor vessel downcomer and cold-legs inlets

Valér Gottlasz[1], Ezddin Hutli[2], Dániel Tar[1], György Ézsöl[1] and Gábor Baranyai[1]

[1] Department of Thermohydraulics, Centre for Energy Research, Hungarian Academy of Sciences, Budapest, Hungary
[2]PhD, Faculty of Mechanical engineering, Belgrade University, Thermo-hydraulics department - Centre for Energy Research, Hungarian Academy of Sciences
gottlasz.valer@energia.mta.hu

ABSTRACT

In nuclear power plants (NPP) as operating plants become older, the piping system Tees and the downcomer are susceptible to turbulent temperature mixing effects (thermal fatigue) that cannot be adequately monitored by common thermocouple instrumentation. The work has been initiated at MTA EK where the mixing flow process is investigated in order to reduce the temperature fluctuation, thus decrease the thermal fatigue risk and to improve the accuracy and reliability of thermal fatigue load positions in the system. A model of a part of the downcomer has been built containing three main loop pipes (cold-legs) and one ECCS pipe (branch pipe). The whole model is made of plexi-glass so optical measurements can be performed from any positions. Particle image velocimetry (PIV) and Laser induced fluorescence (LIF) measurements in significant crosssections in addition to FLUENT calulations has been made. The obtained results showed the influence of important parameters on the mixing process, the ratio of flow rate between the main pipe and the branch pipe has big infelunce on the mixing process, the existence of eblow configuration enhances the mixing flow process in the system. The compariosn bewteen PIV, LIF and FLUENT results shows a good agreements. Both PIV and LIF techniques can be used as good providers for data base and to validate CFD results.

1. Introduction

Currently, many nuclear reactors worldwide are nearing or reaching their originally prescribed lifetime of approximately 40 years. In response, there are initiatives to address the main problems that limits this lifetime so that existing power plants can be safely kept in operation for longer (up to 60 years) and new power plants can be designed with a longer lifetime. One of these major problems is the phenomenon of thermal fatigue, which is defined as a failure caused by thermal stress. It is an important phenomenon in nuclear power plant management considerations and safety assessment. After many thermal fatigue events that have recently occurred in various nuclear power plants the focus of thermal striping studies included both fast breeder reactors (FBR) and light water reactors [1-3].
The service inspections in NPPs reveal that thermal fatigue cracks may occur in welds and base material, straight pipes and elbows. The severity of the failure is dependent on the shape of the component, the fluid mixing mechanism, and the temperature distribution. These effects have been attributed to thermal temperature stratification and turbulent mixing effects caused by different mass flows in “main” and “branch” pipes merging at the Tees connections. Good examples of thermal fatigue events in nuclear power plants are the French FBR in 1992 and PWR in 1998, the Japanese PWR in 1999 and in 2003. [1, 3, 4]
The high cycle turbulence effects are not appropriately detectable by common thermocouple instrumentation thus we need to find another suitable tool to detect the turbulence effects. Because of the lack of thermocouples many researchers investigated the thermal fatigue phenomenon and the related factors numerically and/or experimentally based on the fluid mixing phenomena in the T-junction and its effects on the mixing mechanism in complex system in power plant [5-12].High techniques such as PIV technique associated with the thermocouples network were also used in this field [2, 13-16].
In this paper the flow field and the temperature differences near the downcomer cold-leg inlets and at the ECCS T-junction have been measured illustrated and quantified by experimental and numerical approaches on the test model (the half of the downcomer is modelled by a rectangular tank) using PIV, PLIF, and CFD. The measurements have been performed on plexi-glass mock-up in various positions. The CFD calculation has been done under the same conditions. The T-junction was selected because it is a common component in the cooling systems of most nuclear power plants that has a high capability of thermal fatigue. The comparison has been done between the results obtained by PIV, PLIF, and CFD. In order to investigate the influence of elbow configuration on the mixing process, the flow behavior in two

main pipes were tested but only the results related to the main pipe with elbow configuration are presented here because of the limited space.

2. Facility and Experimental part

The real pressure vessel and the downcomer is cylindrical (Fig. 1a). In order to use the symmetry in our model the downcomer is turned into a plane sheet. One half of the downcomer is modelled by a rectangular tank. Three pipes connecting to this tank modelling the cold-legs. There is a smaller pipe joining to one of these pipes. This smaller pipe is modelling the ECCS inlet mimicing the VVER-440 reactors geometry. The whole model is built of plexi-glass so it's optically measurable. The geometry is on Fig. 1(b, c). Table 1 presents the geometrical properties of the model and the real NPP. Table 2 presents the flow conditions for the model and for also the real NPP.
In this work, a 2D-PIV, PLIF technique were used to measure the flow field and temperature distribution. The advantage of using PIV and LIF techniques is that the flow does not get disturbed during the measurements (there are no effects on the flow characteristics). The experimental conditions are presented in Table 2. The temperature difference between two pipes was fixed at 20 ^{o}C (40 ^{o}C in the main pipe and 20 ^{o}C in the branch pipe). The tested parameters are given in Table 3. PIV measurements has been done in many cross section as shown in Fig. 2, the reason for focusing on the area of the T-junction at the ECCS and the cold-leg and the "T-junction" at the cold-leg and the downcomer is that the mixing process at these positions have a large effect to the thermal fatigue. The temperature differences at Tees have been measured, illustrated and quantified by experimental and numerical approach on Tee-test model in various positions (Fig. 2) and configurations using PLIF and CFD. The Computational Fluid Dynamics (CFD) - codes have been used to simulate the turbulent fluid behavior, in particular, to find the velocity field and temperature distribution in the fluid at same areas of experimental work. The CFD-approach has been validated by a benchmark calculation compared to experimental test results. Guide-lines will be developed from the experimental and numerical results to provide a validated basis for future CFD-calculations of pipe systems in NPP.

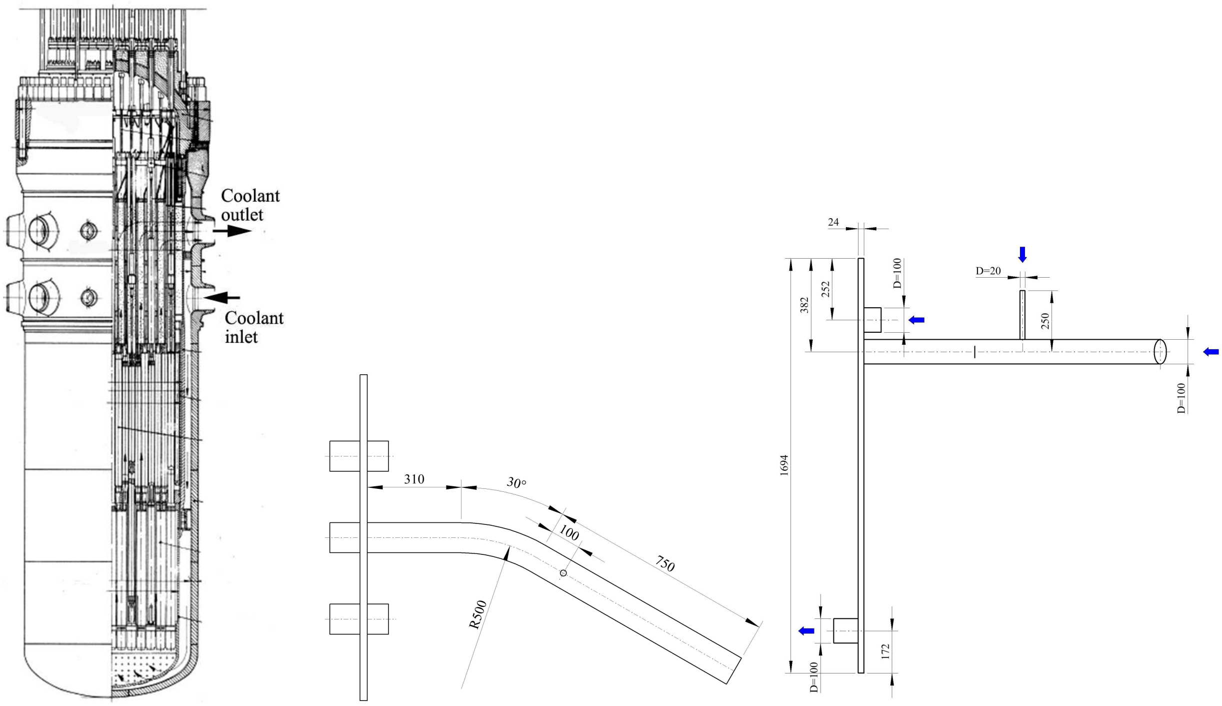

(a) (b) (c)

Figure 1 (a) - typical geometry of VVER – 440 pressure vessel [17], (b, c) – inner dimensions of the geometry

Table 1 Geometry of parts of the Paks NPP and the used Model

Geometry part	Paks NPP	Model
Diameter of the cold-leg	492 mm	100 mm
Size of the "half" downcomer (width x depth)	5376x121 mm	1080x24 mm
Height of the downcomer	7710 mm	1554 mm
D-C hiegth above the inlet	987 mm	249 mm
Inner diameter of the ECCS pipe	111 mm	22 mm
ECCS nozzle position from the inner wall of the DC	3350 mm	670 mm
Length of the cold-legs	-	2000 mm

Table 2 Experimental conditions for PIV, LIF meauserments and CFD calculations

Condition name	Cold-leg flow rate (each pipe) (Q) [m^3/h]	ECCS pipe flow rate (q) [m^3/h]	Flow rate ratio (FRR%) (q/Q)*100	Cold-leg temperature [ºC]	ECCS temperature [ºC]
A	6.3	2.6	42%	40	25
B	6.3	1.6	25.4%	40	20
C	3.2	1.6	50%	40	20
D	3.2	0.8	25%	40	20

2.1. PIV and PLIF procedures

PIV measurements were done with micro size particles dispersed in the fluid of ionized water. In LIF measurements fluorescent dye (Rhodamine B) is dissolved in to the fluid flow. In order to have precise results of PIV measurement the scaling factor calibration has been applied for the determination of the absolute velocities, in case of LIF measurement the intensity-temperature calibration for each pixel is essential. In PIV measurements the diameter of the polyamide seeding particles was 20 μm and their density was 1.016 g/cm^3, which was equal to the water density. Thus the velocity of the particles represents the velocity of the coolant. Because of the difficulty to fully understand the mixing flow process and its mechanism through the mere visualization of the entire flow field small regions around the Tee junctions were selected to more efficiently measure close-up flow-field data. This visualization displays origins of the velocity and temperature fluctuations in the T-junction area. The typical investigation (interrogation) area size was 16×16 pixel, and cross correlation was used for the calculation. The time between the two laser impulses was set to 100-200 μs depending on the flow conditions. The time averaged velocity field results have been obtained by recording 500-1000 frame pairs at 2 Hz frequency. The energy of the Nd YAG laser was set to 20% of the maximum 50 mJ, the repetition rate was the same of the 2M CCD camera. Over the Flow-map system we process the results via Flow-manager software and Matlab 2012.

Table 3 Testing parameters in PIV, LIF measurements and CFD calculations

Parameter name	**Paks NPP**	**Model**
Cold-leg flow rate	300 kg/s	0,5 – 3 kg/s (per loops)
ECCS flow rate	28 kg/s	0,01 – 1 kg/s
Cold-leg temperature	267 C^{o}	40 C^{o}
ECCS temperature	55 C^{o}	20 C^{o}

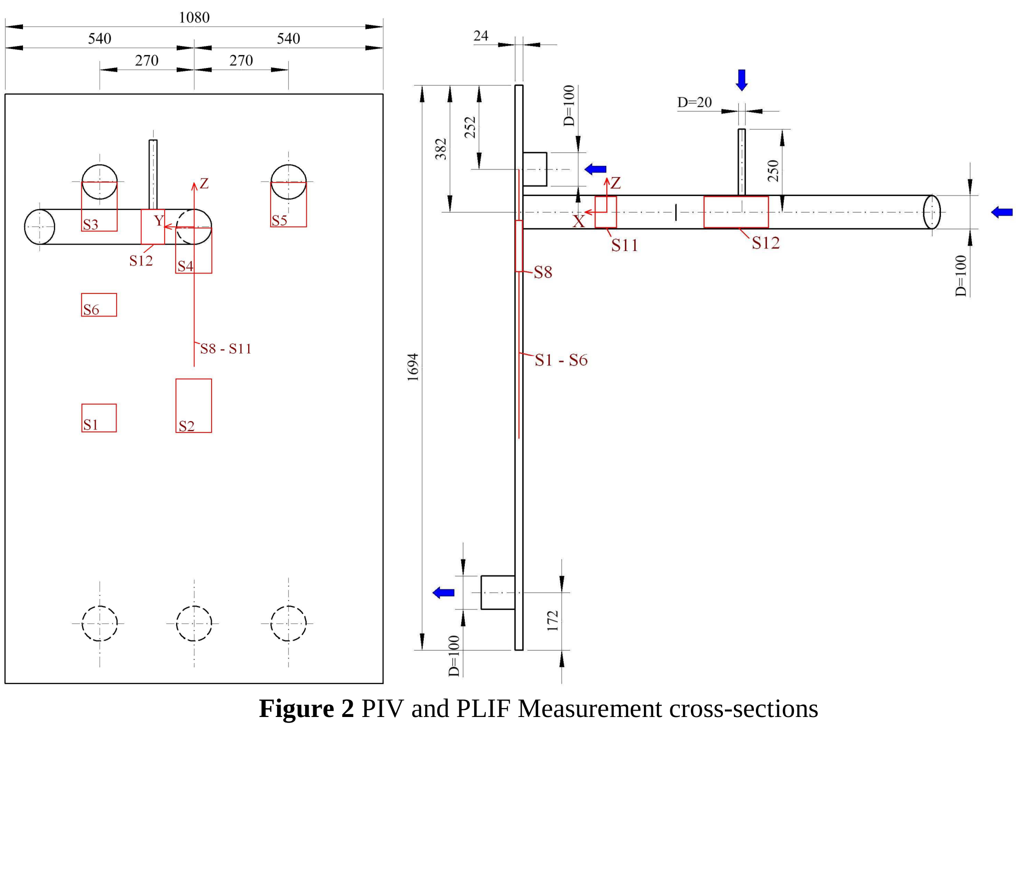

Figure 2 PIV and PLIF Measurement cross-sections

For the different cross-sections different measurement arrangements are necessary. Fig. 3 shows the setup of the tools (camera and the laser) to perform the measurements at S4, S8 and S12cross-sections respectively.

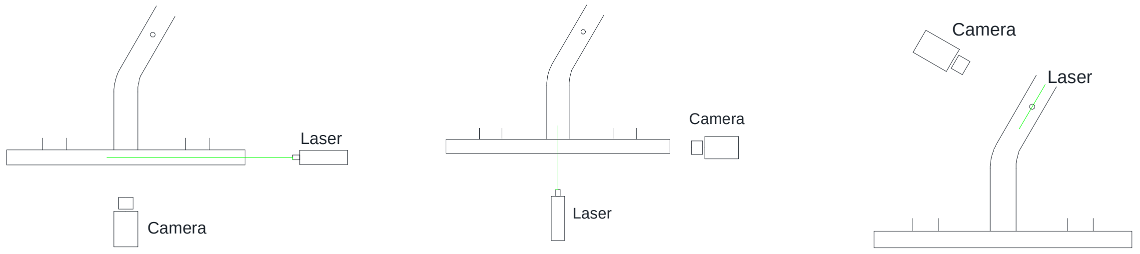

Figure 3 PIV and LIF visualization system arrangements

3. Results and discussion

3.1. PIV and PLIF procedures

The flow visualization test in the T-junction using PIV technique was carried out with parameters related to flow rate ratio (FRR) between two pipes (branch and main pipe as in Table 2). As it was mentioned earlier it is difficult to fully understand the mixing mechanism of the fluid through the mere visualization of the entire flow field, therefore a small region around the T-junction was selected to measure close-up flow-field data (PIV, PLIF and CFD has been made on the same region). This visualization displays origins of the velocity fluctuations in the T-junction area.

Fig. 4(a, b, c) shows the mean flow pattern (mean velocity vector map) in the T-junction which is characterized by the jet behavior exiting from the branch pipe. The used working conditions are A, C, and D (Table 2). The jet was bent in the direction of the main flow of the main pipe (effect of high upstream flow velocity of the main pipe). With increasing the flow rate of the main pipe the bend of the jet increase i.e. jet penetration decrease. The jet penetration depends also on the flow rate of the branch pipe itself [2, 13]. But in general the expected forms of the jet depend on the flow rate ratio between both pipes (*FRR = (q/Q)*100 %*). This could be classified into four patterns; (1) wall jet (low flow rate ratio, not presented here), (2) re-attached jet, (3) deflecting jet (flow rate ratio as it given in Table 1, is presented here), and (4) impinging jet obtained by the increasing flow in the branch pipe, thus depending on the momentum/velocity ratio of the entering flows from branch and main pipe, the turbulent mixing patterns can be classified and defined clearly. The existing elbow after the T-junction (branch pipe) and before the downcomer entrance (T-junction at the downcomer) enhances the mixing process [2, 13, 16].

Three parameters are used to investigate the structure of the jet and mechanisms: mean velocity distribution in x and in z-direction plus velocity fluctuation. The mean velocity distribution contains information about the average structure of the jet, while, the velocity fluctuations display the area with the highest variation (not presented here) but it could be understood from velocity vector map in Fig.4(a, b, c). For each condition 1000 frames were used to evaluate the mixing flow mechanism and mean velocity. This is the reason why we did not see any kind of vortices on the velocity vector map (we present average). The influence of the flow rate of the branch pipe on the mixing process can be understood from the comparison between the results obtained with condition (C) and that with condition (D) (Fig. 4(b) and Fig. 4(c)) shows that the jet thickness and penetration increase as the jet flow rate increases. The bending of the jet by main flow coming from the main pipe decreases with the increase in the jet flow rate.

Fig. 5 and Fig.6 show the comparison between the velocity profiles in x-direction and in z-direction extracted from PIV and CFD results at certain cross-sections. The comparison shows good agreements.

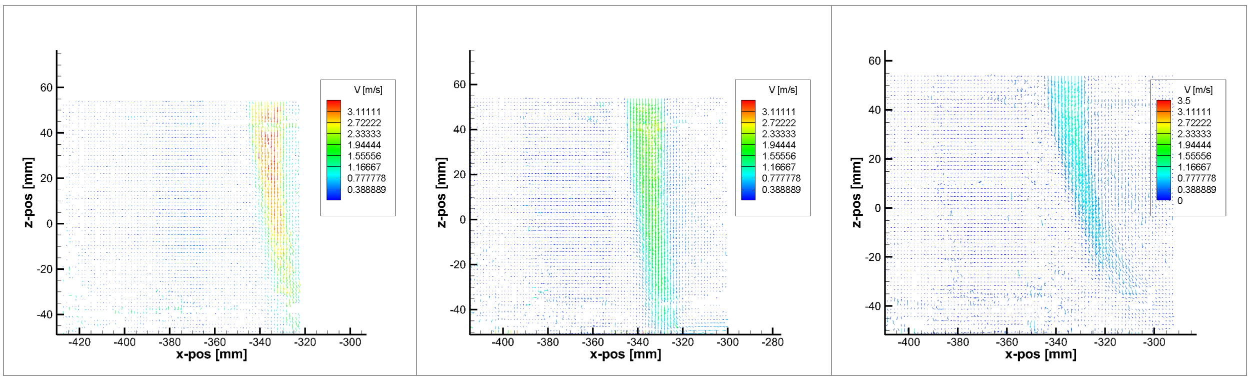

(a) (b) (c)

Figure 4 PIV velocity distributions [m/s] obtained under working conditions A, C, and D respectively

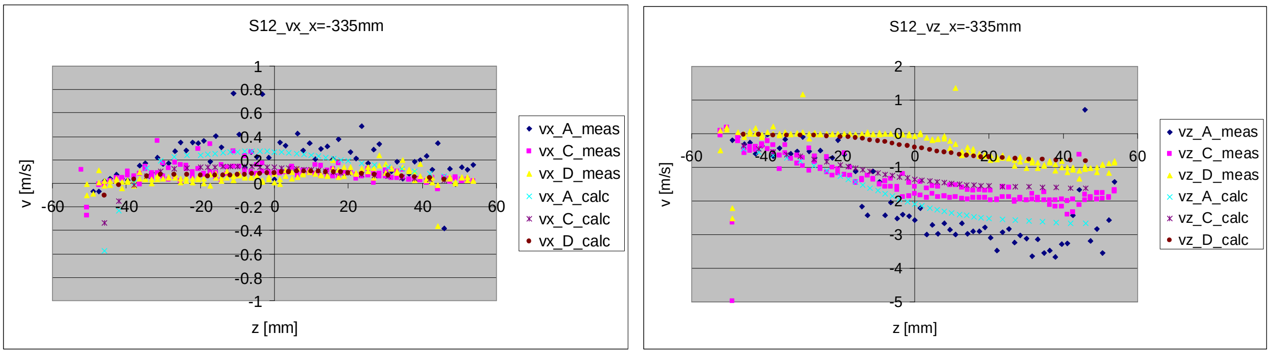

Figure 5 profiles of the velocity-components in x direction (PIV and CFD)

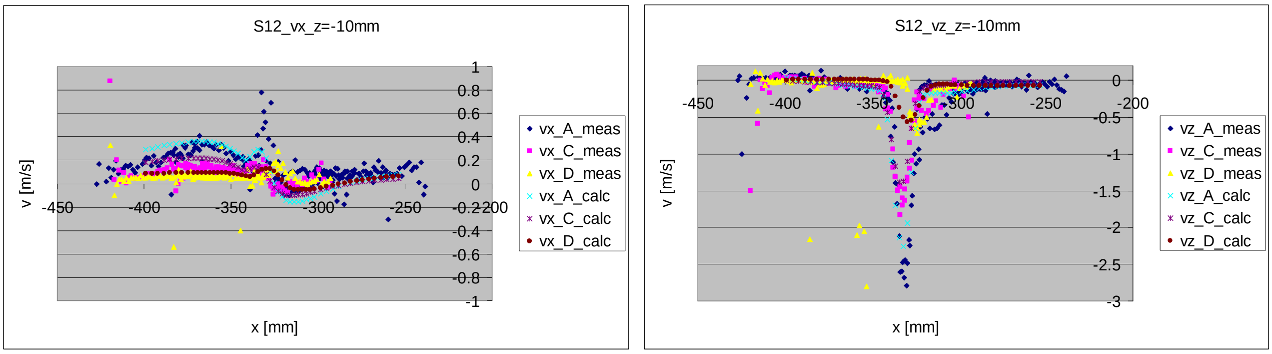

Figure 6 profiles of the velocity-components in z direction (PIV and CFD)

Fig. 7(a, b, c) shows the mean velocity vector map obtained by PIV measurements at cross-section S8 in the T-junction at the downcomer entrance under three different working conditions (A, B, and C respectively). From Fig. 7(a) and Fig. 7(b) we can deduce the influence of branch pipe flow rate on the velocity distribution at the downcomer inlet. The flow rate was changed for each case (see Table 2.).

The analysis of the two vector maps (Fig. 7(a) and Fig. 7(b)) reveals that the ratio between the two flow rates has significant influence on the velocity distribution i.e. on the mixing process; in other words the flow rate of branch pipe has significant influence on the flow characteristics when the other parameters are kept constant. The highest velocity is recorded on left side as it appears in both Fig. 7(a) and Fig. 7(b), this assymmetrical distribution is a result of the elbow configuration in the main pipe (Fig. 1(a)). In general the mean velocity is high in the T-connection in the lower arc of the main pipe (fluid shedding area) and in the border under the arc. This is also related to the elbow configuration in the pipe.

The comparison between Fig. 7(b) and Fig. 7(c) shows the influence of the main pipe flow rate. The flow rate ratio for condition B (Fig. 7(b)) was $FRR = (q/Q)*100\%$ = 25.4% while for condition C (Fig. 7(c)) it was FRR = 50%. The comparison reveals that the increase in the flow rate ratio is enhancing the mixing process. This fact could be read from the distribution of the velocity on Fig. 7(b) and Fig. 7(c). The velocity distributions are more homogeneous in Fig.7(c) than in Fig. 7(a) and Fig. 7(b). From these results we can say that there is an optimum *FRR* which can lead to get high mixing rate i.e. optimum velocity distribution. In other words the design is intended with respect to the mixing process. *FRR* (as in its definition) depends on the flow rate of both pipes (main and branch pipe) and the flow rate is a function of the velocity and the diameter.

Fig. 8 and Fig. 9 show the velocity profiles of Vy obtained by PIV measurement results and calculated using CFD. The agreements are clear between these results; the existence of deviation in some points could be acceptable because the flow is complex the error could come from both techniques (PIV and CFD). This deviation needs further investigation. As mentioned in the publications the discrepancies could be due to the integrated effects of many complex flow phenomena such as wake-wake, wake-vane, and vane-boundary layer interactions occurring simultaneously in complex flow environment [18]. Both the repetition of the calibration process and the measurements (average should be used) were necessary in this work to get results with high accuracy.

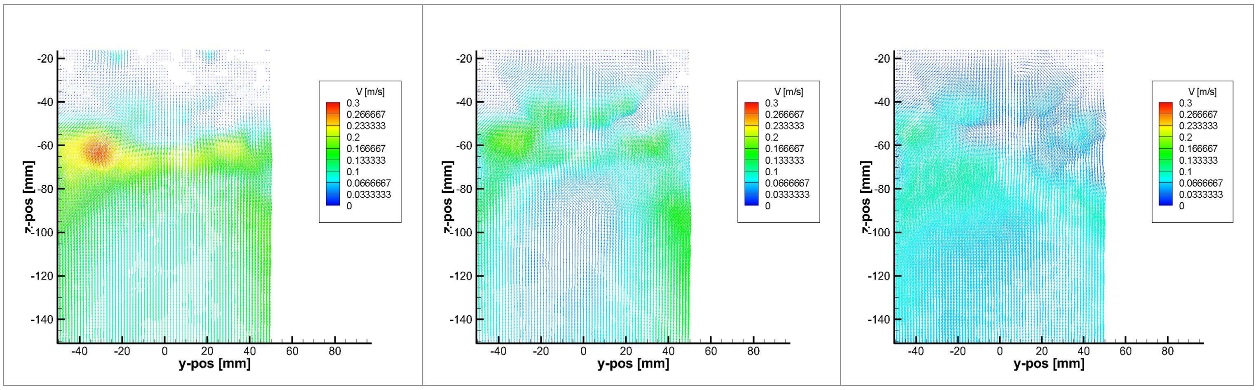

(a) (b) (c)

Figure 7 PIV velocity distributions [m/s] obtained at S4 position under working conditions A, B, and C respectively

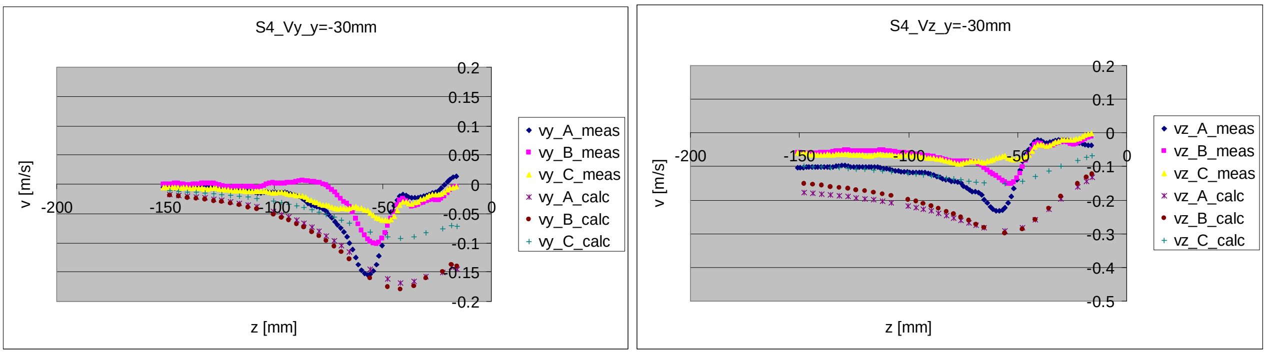

Figure 8 profiles of the velocity-components in z direction on the left side of the inlet of the downcomer at the main pipe (PIV and CFD)

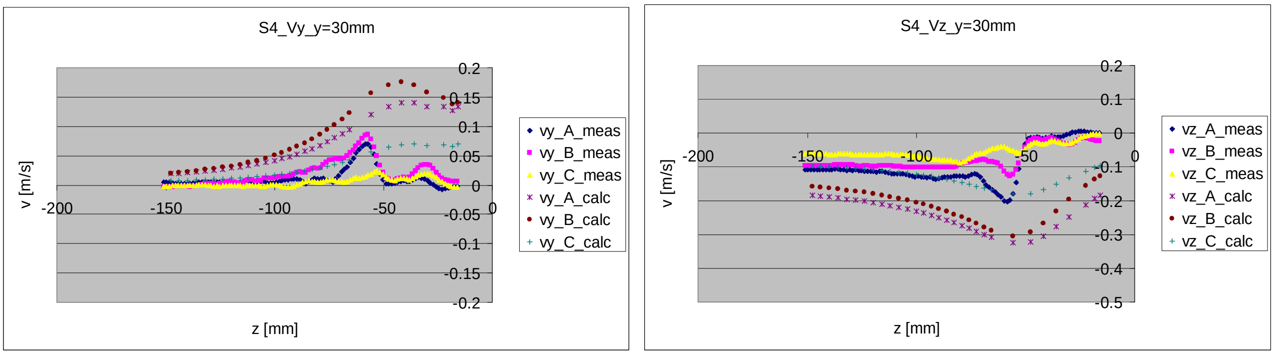

Figure 9 profiles of the velocity-components in z direction on the right side of the inlet of the downcomer at the main pipe (PIV and CFD)

Fig. 10(a, b, c) show the results obtained by PIV measurements at S8 under the conditions A, B, and C respectively. The influence of the flow rate of both pipes and flow rate ratio on the velocity distribution could be understood by comparing the velocity victor maps in Fig. 10 (a, b, c). The comparison between the PIV and CFD results show a good agreement as shown in Fig.11.

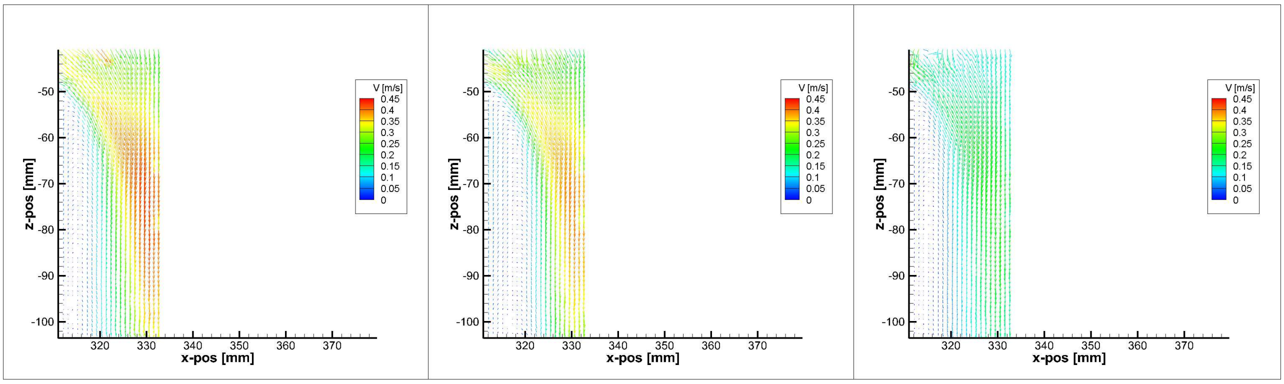

(a) (b) (c)

Figure 10 PIV velocity distributions [m/s] obtained at S8 position under working conditions A, B, and C respectively

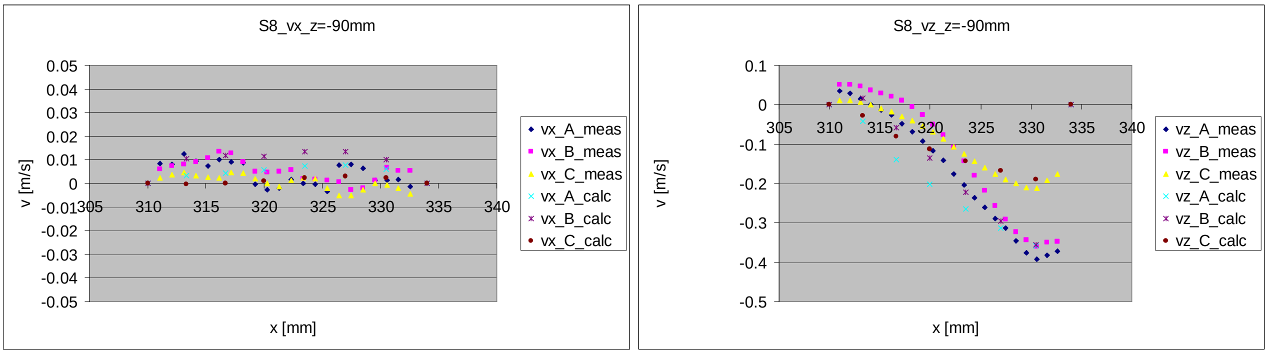

Figure 11 profiles of the velocity-components in x and in z direction (PIV and CFD)

3.2. PLIF Temperature Measurements and CFD calculations

The temperature differences at Tees have been measured using PLIF, illustrated and quantified by experimental approaches on Tee-test models in various positions and configurations and CFD calculations were made under the same conditions. The presented results here are the average of a few hundred measurements (frames) for each working condition and CFD outputs. Thus the expected errors are eliminated. The PLIF measurements and the CFD calculations have been done under four working conditions in order to investigate the influence of the FRR and the flow rate of both branch and main pipe on the mixing flow process. The temperature distribution is used as an indicator for the quality of the mixing process. The measurements and calculations have been made based on inlet velocities (flow rates) and temperatures as given in Table 2.

The main pipe has a mixing elbow configuration after the branch pipe which is commonly used in piping systems for power plants and process industries. The elbow is used to bias the velocity distribution and also to have an effect on the secondary flow, which decays unsteadily, i.e. enhance the mixing phenomenon that already started between the fluids caming from the two pipes (the T-junction), thus the fluid will be homogenized thermally before the downcomer entrance. This elbow configuration has effect on the interaction between the jet and the main flow even it is after the T-junction between branch and main pipes because of the deflected fluid from the corner of the elbow. The significant effect of elbow appears clearly in the velocity and temperature distribution and profiles measured after elbow [2, 13, 16].

Fig.12 and Fig.13 show the PLIF and CFD results respectively obtained under working conditions A, B, and C (Table 2) (note the CFD results are mirrored). The comparison between PLIF and CFD shows high correlation in respect to the temperature distribution in the tested area. From the results of both PLIF and CFD techniques the highest temperature appears around the jet. In the bottom we can see the middle (mixed) temperature value recorded, as a result of the jet penetration. The mixing area in the images is the area which has middle temperature values according to the scale associated with each image in Fig. 12 and Fig.13. As a result of the temperature difference between the branch pipe the main pipe the average structure of the jet could be noticed easily. By decreasing the flow rate of the branch pipe (condition B in Table 2.) the flow from the main pipe bent the jet which in turn dercreased the jet penetration. Again comparison between PLIF and CFD results shows a good agreement.

Comparison between Fig. 12(a), Fig. 12(b), Fig. 13(a) and Fig. 13(b) gave highlights about the influence of the flow rate of the branch pipe on temperature distribution and the mixing flow process.

Fig. 12 (c) shows the results obtained with working condition C (Table 2.). In this figure the jet appears with less bent because the flow from main pipe is decreased. Fig.12 (b), Fig.12(c), Fig. 13(b) and Fig. 13(c) give the highlights of the influence of the flow of the main pipe on the temperature distribution and mixing phenomenon in the tested area.

The analysis of the results in Fig.12 (a,b,c) and Fig.13(a,b,c) reveals that the momentum ratio between the main velocity and the branch velocity of the mixing tee is the most useful parameter for classifying the fluid mixing mechanism, which includes both the velocity and pipe diameter characteristics of the main and branch pipes. In addition, the effects of flow rate (velocity when diameter is kept constant) on the fluid mixing mechanism shown and explained the behavior of turbulent jets.

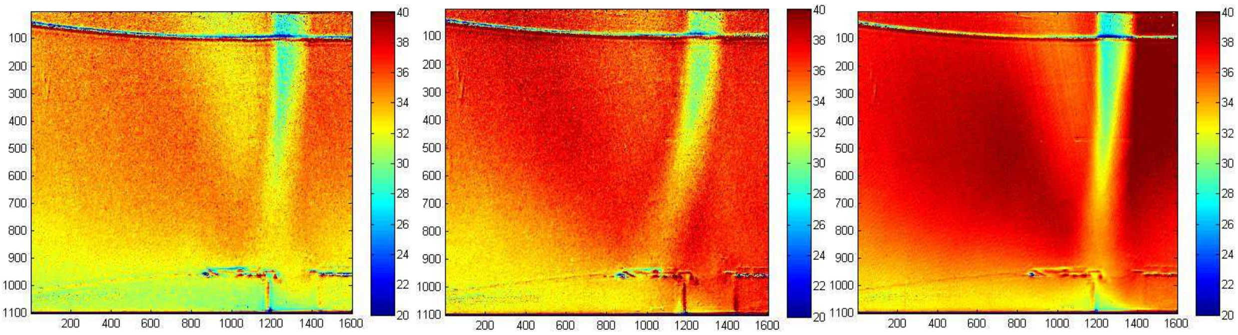

(a) (b) (c)

Figure 12 PLIF temperature distribution [m/s] obtained at S8 position under working conditions A, B, and C respectively

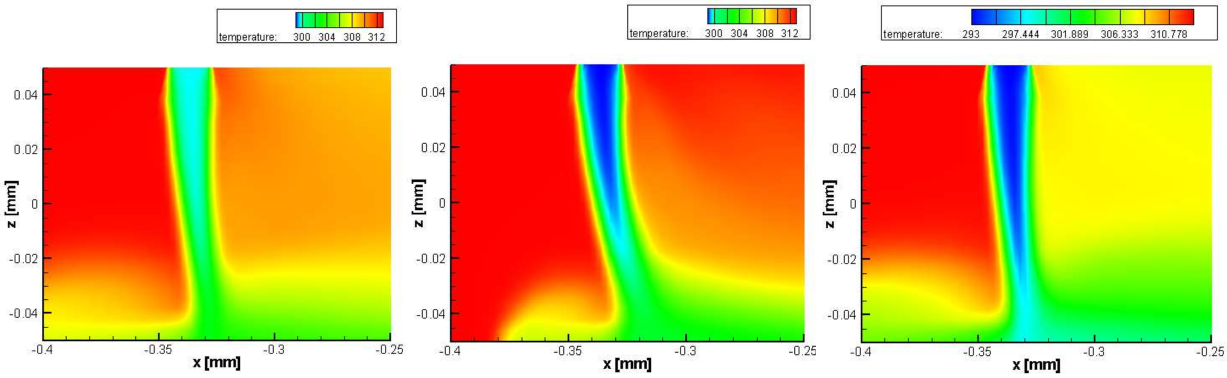

(a) (b) (c)

Figure 13 CFD temperature distribution [m/s] obtained at S8 position under working conditions A, B, and C respectively

4. Conclusion

A water experiment using a VVER-440 downcomer which is modelled by a rectangular tank, simple T-pipe junction with downstream elbow in the main pipe was carried out to investigate thermal striping phenomena. Fluid temperature and velocity distributions in the pipe and in downcomer were measured using PIV, LIF system and CFD calculations were performed. The results showed that the flow pattern in the downcomer – cold-leg T-junction was characterized by the branch pipe jet which acts as a turbulent jet in the connecting main pipe. Various types of jets could appear, depending on the flow rate ratio when the pipe's geometries were kept constant. The flow rate ratios between between the main and the branch pipe were selected to study the mixing flow process before the entrance of the downcomer in order to minimize the thermal fatigue risk. Different operating hydrodynamical and gemetrical conditions in the T-junction areas were introduced. The infelunce of the elbow configuration in the main pipe has significant infelunce on the mixing phenomenon (on velocity and temperature distribution). By optomising the flow rate ratio of the piping system the temperature fluctuation in the mixing tee can decrease significantly thus reduce the thermal fatigue risk. The PIV and LIF measurement technology proved to be suitable for the investigation of the turbulent mixing phenomenon in the complicated piping system geometry. Comparison of PIV, LIF measuerments and CFD calculation results showed a good quantintive and qualtiative agreement thus they could be good providers for CFD validation.

REFERENCES

[1] K-J. Metzner K.J. et al "Thermal Fatigue Evaluation of Piping System "Tee"—Connections (THERFAT)" (2007)

[2] Hosseini S. M., Yuki K., Hashizume H. "Classification of Turbulent Jets In A T-Junction Area with a 90-Deg Bend Upstream" International Journal of Heat and Mass Transfer 51 (2007) pp, 2444–2454

[3] IAEA-TECDOC-1627 “Pressurized Thermal Shock in Nuclear Power Plants: Good Practices for Assessment, Deterministic Evaluation for the Integrity of Reactor Pressure Vessel” INTERNATIONAL ATOMIC ENERGY AGENCY -VIENNA (2010)

[4] Eggertson, E.C. Kapulla, R, Fokken, J, Prasser, H.M. “Turbulent Mixing and its Effects on Thermal Fatigue in Nuclear Reactors” World Academy of Science, Engineering and Technology 52 (2011) pp. 206-213.

[5] S.M. Hosseini “The three-dimensional study of flow mixing phenomenon” International Conference Nuclear Energy for New Europe ID: 037, Bled, Slovenia (2005)

[6] C. Faidy “Thermal Fatigue In Mixing Areas: Status And Justification Of French Assessment Method” Third International Conference on Fatigue of reactor Components, EPRI-US NRC-OECD NEA, Seville, Spain (2004)

[7] Muramatsu, T. “Numerical Analysis of Nonstationary Thermal Response Characteristics for a Fluid-Structure Interaction System” Journal of Pressure Vessel Technology, 121 (1999) pp.276-282

[8] Garashi, M., Tanaka, M., Kimura, N., Kamide, H. “Study on Fluid Mixing Phenomena for Evaluation of Thermal Striping in a Mixing Tee” NURETH10, NURETH10-A00512 (2003)

[9] M. Igarashi “Study on fluid mixing phenomena for evaluation of thermal striping in a mixing tee” 10th International Topical Meeting on Nuclear Reactor Thermal Hydraulic, NURETH-10, Seoul, Korea (2003)

[10]M. Tanaka “Experimental Investigation of Flow Field Structure in Mixing Tee” Proceedings of Sixth International Conference on Nuclear Thermal Hydraulic, Operation and Safety, ID: N6P334, NUTHOS-6, Nara, Japan (2004)

[11]S.M. Hosseini “Experimental investigation of thermal-hydraulic characteristics at a mixing tee” International Heat Transfer Conference, FCV-17, Sydney, Australia (2006)

[12]Kimura N., Nishimura M., Kamide, H. “Study on Convective Mixing for Thermal Striping Phenomena – Experimental Analyses on Mixing Process in Parallel Triple-Jet and Comparisons between Numerical Methods” ICONE9, No.4. (2001)

[13]Ogawa H., Igarashi M., Kimura, N., Kamide H. “Experimental Study on Fluid Mixing Phenomena In T-Pipe Junction With Upstream Elbow” The 11th International Topical Meeting on Nuclear Reactor Thermal-Hydraulics (NURETH-11) Popes Palace Conference Center, Avignon, France (2005)

[14]Hosseini S.M. “Visualization of fluid mixing phenomenon” Sixth International Congress on Advances in Nuclear Power Plants, ICAPP05, ID: 5006 (R006), Seoul, Korea, (2005)

[15]Aminia N., Hassan Y.A. “Measurements of jet flows impinging into a channel containing a rod bundle using dynamic PIV” International Journal of Heat and Mass Transfer 52 (2009) pp. 5479–5495

[16]Fluent Inc. FlowLab 1.2 “Turbulent Flow and Heat Transfer in a Mixing Elbow” (2007)

[17]Gango P. “Numerical boron mixing studies for Loviisa nuclear power plant” Nuclear Engineering and Design 177 (1997) pp. 239–254.

[18]Elvis E. D.O., Yassin A. H., Michael E.C., Zeses K. “Experimental Benchmark Data for PWR Rod Bundle with Spacer-Grids” Proceedings of the CFD for Nuclear Reactor Safety Applications (CFD4NRS-3) Workshop, Bethesda North Marriott Hotel & Conference Centre, Bethesda, MD, USA (2010)